JEVA

JOURNAL OF ELECTRONIC VOLTAGE AND APPLICATION
e-ISSN: 2716-6074

Vol. 7 No. 1 (2026) 28-43
https://publisher.uthm.edu.my/ojs/index.php/jeva

Detection Method for Authenticity Assessment of Malaysian Tualang Honey Using Absorbance and Transmittance Analysis with combination of Application of Artificial Neural Network - Optical Properties (ANN-OP) Classification

Mohd Hazlan Zakaria[1], Muhammad Mahadi Abdul Jamil[1]*, Wan Suhaimizan Wan Zaki[1], Ariffuddin Joret[1], Noor Azwan Shairi[2]

[1] *Faculty of Electrical and Electronic Engineering, Universiti Tun Hussein Onn Malaysia, 86400 Parit Raja, Batu Pahat, Johor, MALAYSIA*

[2] *Faculty of Electronic Engineering and Computer Engineering, Universiti Teknikal Malaysia Melaka, 76100 Durian Tunggal, Melaka, MALAYSIA*

*Corresponding Author: mahadi@uthm.edu.my
DOI: https://doi.org/10.30880/jeva.2026.07.01.004

Article Info

Received: 26 June 2025
Accepted: 14 April 2026
Available online: 30 June 2026

Keywords

Pure honey, diluted honey, absorbance, transmittance, wavelength, optical system

Abstract

Honey is a highly valued natural sweetener, frequently subjected to adulteration due to its economic importance. It is commonly consumed for its perceived health benefits and as a substitute for refined sugar in a wide range of food products. In Malaysia, the widespread availability of diluted honey poses a significant challenge in distinguishing between pure and adulterated forms. This study presents a simple spectrophotometric approach using absorbance and transmittance measurements to differentiate honey authenticity. Eight honey samples, both pure and adulterated, were analysed. Results showed that the darker honey samples exhibit higher absorbance values, while lighter samples demonstrate faster signal responses in transmittance measurements. Optimal wavelengths were identified at 480 nm for absorbance and 630 nm for transmittance. These wavelength-specific responses provide an effective means of identifying adulterated honey. This method offers a practical solution for consumers and industry professionals seeking to verify honey purity, especially for health and dietary applications.

1. Introduction

According to the World Honey Market, “Adulterated honey ultimately robs consumers of the natural health benefits found in pure raw honey. For more than 10,000 years, as civilizations rose across the earth, honey has been prized for its medicinal properties” [1]. However, widespread adulteration has diminished these benefits, driving down honey prices, disrupting the industry, and reducing the number of natural honeybee colonies available in the market. From 2007 to 2019, global exports of Asian honey increased by 128 %, despite only a slight increase in the number of beehives and declining honey yields due to threats such as pesticide exposure,

nutritional deficiencies, and parasitic mites [2]. This discrepancy suggests potential issues in honey authenticity and purity, reinforcing concerns over adulteration.

Pure honey is widely recognized for its exceptional protective effects against oxidative stress in the human body and the oxidation of food. Historically, even thousands of years ago, honey was used to treat a variety of human ailments [3], [4]. It was believed that honey's healing properties stemmed solely from its natural composition. With technological and medical advancements, modern research has increasingly revealed the remarkable properties of honey and its complex biochemical composition. Antioxidants are among the most significant components of honey, known for neutralizing the harmful effects of free radicals [5].

Although the health benefits of honey are well established, a major challenge in Malaysia lies in verifying the authenticity of honey sold in the market. Many consumers trust local honey sold by indigenous communities, assuming it to be pure. While this may sometimes be true, it is not always the case. A study by Yusoff et al. [6] found that 31 out of 40 Malaysian honey samples analysed for sugar content and hydroxymethylfurfural (HMF) levels were either adulterated or synthetic. Alarmingly, some samples falsely labelled as "pure" honey were also obtained from indigenous sources. Such misrepresentation constitutes a violation of consumer rights, potentially causing physical harm or psychological distress.

Numerous studies have aimed to differentiate between pure and adulterated honey using various analytical techniques. These include Fourier-transform infrared spectroscopy (FTIR), near-infrared spectroscopy (NIR), internal standard carbon isotope ratio analysis (ISCIRA), nuclear magnetic resonance (NMR), high-performance liquid chromatography (HPLC), and gas chromatography-mass spectrometry (GC-MS) [7]-[11]. While these methods offer high accuracy, they are often time-consuming, costly, require complex sample preparation, and demand skilled personnel.

Additionally, biomimetic sensors such as the electronic nose (e-nose) and electronic tongue (e-tongue) have shown promise by detecting specific aroma and taste profiles of honey. However, effective differentiation among honey types using these sensors often requires data fusion and advanced multivariate analysis [8]. Therefore, the development of simple, rapid, and cost-effective screening methods for assessing honey authenticity is crucial. Ensuring the purity of Malaysian wild honey will enhance its credibility and competitiveness in both local and international markets, reinforcing its status as a premium product in the healthy food industry.

2. Related Works

Recent studies have explored the application of fibre optic displacement sensors (FODs) for evaluating the purity of local honey samples [11]. These sensors detect variations in output signals corresponding to different glucose concentrations in honey, thereby distinguishing pure honey from adulterated variants. Sensor calibration was initially performed in a quartz cell without a sample to establish a baseline. Experimental results indicated that the sensor exhibited maximum sensitivity at 10% adulteration and minimum sensitivity at 0%, i.e., pure honey. This highlights the sensor's ability to detect low concentrations of adulterants, making FODs-based transmission techniques a promising candidate for real-time honey purity assessment. The sensing configuration employs a bifurcated optical fibre system: one fibre transmits light from a 457 nm blue diode laser, and another receives the light after it has passed through the honey sample. The laser source is modulated externally at 150 Hz to avoid interference from ambient light and harmonics of the 50–60 Hz power frequency. A lock-in amplifier is used to suppress DC drift and minimize noise. The honey sample is held in a 10 mm quartz cell positioned between the fibre ends. Light scattered and refracted by the honey sample is collected via the receiving fiber and directed to a photodiode detector for intensity measurement. This setup enables precise monitoring of optical changes in the sample, which correspond to its purity level. The sensor demonstrated a sensitivity of 32.65 mV/mm and a linearity of 99%, validating its potential as a simple and cost-effective alternative to complex chemical testing methods [11]. Its minimal sample preparation, reusability, and non-destructive nature make it suitable for application in the food industry, particularly in detecting glucose adulteration in honey.

Beyond fibre optic sensing, spectroscopic techniques have also been widely used in honey authentication. Spectroscopy, which involves the interaction between electromagnetic radiation and matter, can provide valuable information on the chemical composition of honey. Techniques such as nuclear magnetic resonance (NMR), Raman spectroscopy, and infrared spectroscopy (IR) have proven effective in quantifying sugar profiles [12] and determining the geographical origin of honey [13]. In particular, Fourier Transform Infrared Spectroscopy (FTIR) combined with statistical tools like attenuated total reflectance (ATR), principal component analysis (PCA), and partial least squares (PLS) has enabled accurate and rapid discrimination between pure and adulterated honey samples [14], [15].

In addition, the Karl Fischer Titration (KFT) method has been employed to assess water content in honey by chemically reacting with water molecules. Studies comparing KFT with refractive index (RI) measurements on over 100 honey samples found that KFT provides higher accuracy and reliability [16][17]. A related study also compared KFT, RI, and the drying method, which involves evaporating moisture under heat. However, this method may cause loss of volatile compounds if parameters are not well controlled [18]. Fibre optic sensors continue to

be among the most effective tools in modern sensing technologies. For instance, a recent study demonstrated the use of an intensity-modulated fibre optic displacement sensor (FODS) to detect honey dilution in distilled water, further validating the versatility of this technique for purity assessment [19][20]. Table 1 provides a comparative overview of these techniques, summarizing their advantages and disadvantages. This table serves as a useful reference for researchers and industry stakeholders seeking effective tools for honey quality assessment.

Table 1 *Comparison of previous techniques used to determine the authenticity of honey originality with their advantages and disadvantages*

No	Methodology	Advantages	Disadvantages
1	Attenuated Determine Hydroxymethylfurfural (HMF)	Attenuated: Provide summary of the instrumental and analytical methods available	
2	Attenuated Total Reflected Fourier Transform Infrared (ATR-FTIR) Spectroscopy combined with Multi-variate statistical techniques	It can be differentiated between authenticate and adulterated IWH	
3	Addition of sugar	Easy, simple process and cheaper in cost.	It can change biochemical and chemical properties i.e. glucose, sucrose, fructose and hydroxymethylfurfural (HMF)
4	Stable Carbon Isotope Ratio Analysis (SCIRA)	Able to detect the honey adulteration with sugar and evaluate indirect adulteration	This method is not suitable for the addition of C3 plant sugar due to the similarities in isotopic composition.
5	HPLC	Short time analysis and low cost	
6	Spectroscopic technique-based o NMR	1. A useful method to quantify the sugar profile. 2. Determine the geographical origin	
7	Fourier transform infrared spectroscopy	1. Discriminate between pure and adulterated simultaneously in a reliable, direct and rapid way. 2. New analytical method and easy to handle.	1. It depends on the method of extracting the pollen from honey. 2. Required skills of a palynologist in interpreting the results
8	DNA Analysis	1. The screening process is done to distinguish the pollen type in honey bees	1. Essentially depends on climatic and environmental conditions
9	Physico-chemical	1. Both function as either honey characterization or an indicator	1. It requires heat pre-treatment in creamy (crystallized) honey before the analysis
10	RI Measurement		1. Loss of water and the empirical formula or conversion table is therefore incorrect for different types of honey
11	Refractometer KFT	1. Reliable method	
12	Drying	1. Volatile compounds in the sample is evaporated.	1. Volatile compounds in honey also may evaporate together with the water, unless the

No	Methodology	Advantages	Disadvantages
			drying parameters are well-chosen.
13	Fibre Optics Sensors	1. Cheaper components. 2. Simple technique 3. Small in size	1. Required special skills to operate equipment and devices
14	Fibre Optics Displacement Sensors (FODS)	1. Cheaper components. 2. Simple technique 3. Small in size	1. Required special skills to operate equipment and devices
15	Optical Microfiber Sensing	1. Cheaper components. 2. Simple technique 3. Small in size	1. Required special skills to operate equipment and devices

In summary, various methods have been developed to detect honey adulteration and determine authenticity, including isotopic analysis, chromatography, spectroscopy, KFT, drying, and fibre optic sensing.

3. Related Works

3.1 Overview of the Whole System

The workflow for honey authentication using UV–Vis spectroscopy and an Artificial Neural Network (ANN) involves a sequential process starting with sample preparation, where honey samples are homogenized and placed into quartz cuvettes for analysis. These samples are then subjected to UV–Vis spectroscopy, which captures both absorbance and transmittance data across a wavelength range of 200–800 nm. From this spectral data, feature extraction is performed to identify key indicators such as absorbance peaks, transmittance ratios, and intensity values at specific wavelengths. These extracted features serve as inputs to an ANN model structured with 3 input nodes, 10 hidden nodes, and 2 output nodes, designed to learn patterns distinguishing pure from adulterated honey. Finally, the model performs classification, outputting whether each sample is authentic or adulterated based on the learned spectral characteristics. The workflow of honey authentication using UV–Vis Spectroscopy and ANN shown in Fig. 1.

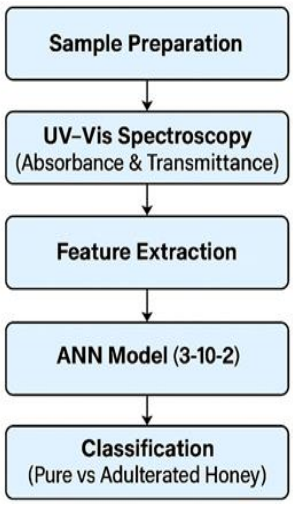

Fig. 1 *The workflow of the honey authentication system*

3.2 Experimental Setup

Authentic Tualang honey was sourced from a reputable bee farm located in Jerantut, Pahang, situated in the central region of Peninsular Malaysia, and used as a reference standard in this study. To investigate the optical characteristics and detect possible adulteration, both pure and adulterated Tualang honey samples were prepared

J. of Electronic Voltage and Application Vol. 7 No. 1 (2026) p. 28-44

in 5 g portions and transferred into quartz cuvettes. Quartz cuvettes were chosen due to their high transparency in the ultraviolet and visible spectral regions, ensuring accurate absorbance measurements across the selected wavelength range.

All samples were analysed using a UV–Vis spectrophotometer at the MINT-SRC laboratory, Universiti Tun Hussein Onn Malaysia (UTHM), operating within a spectral range of 200–800 nm. The spectrophotometer was calibrated using a blank reference prior to analysis to ensure precision. Absorbance data were collected at 1 nm intervals to capture detailed spectral features associated with natural and adulterated honey compositions. In addition to the Tualang honey samples, eight other honey types of varying botanical and geographical origins were similarly prepared and analysed under the same conditions. The resulting spectral data were used as input features for an Artificial Neural Network (ANN) model developed to classify honey samples based on their authenticity.

3.3 Preparation of Honey Samples

Genuine Malaysian Tualang honey sourced from a reputable bee farm in Jerantut, Pahang, situated in the heart of Peninsular Malaysia, was obtained for experimentation to further evaluated and investigated. A total of 30 grams of pure honey and 30 grams of adulterated of honey were distributed evenly into a quartz cuvette container, allowing for 5 grams per compartment. These samples were then tested using a UV-Vis spectroscopy spectrophotometer for both absorbance and transmitted tests at the MINT SRC UTHM lab to get 3 times of measurement for average data consistency. Next, the process of filling the quartz cuvette with various liquids and honey samples such as pure Tualang honey, apple cider, syrup, Gold honey and water to run experiment for both absorbance and transmitted testing. In additional, a series set samples of pure Tualang honey is diluted with 10% of glucose syrup until 100% of glucose syrup to benchmarking pattern of graphical analysis as calibration purpose which were loaded into the quartz cuvette after being analysed using the UV-Vis spectroscopy.

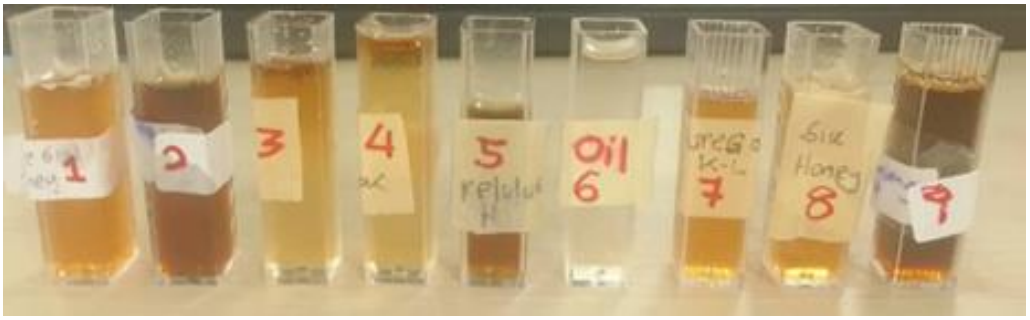

Fig. 2 *All samples of honey have been filled inside a quartz cuvette*

3.4 ANN Model Design

An Artificial Neural Network (ANN) was constructed to classify honey samples as either authentic or adulterated based on their UV–Vis spectral data. The network architecture consisted of three input nodes, representing selected spectral features such as absorbance peaks, transmittance ratios, and wavelength-specific intensity values. These inputs were processed through ten hidden nodes, which enabled the model to perform pattern recognition and learn complex relationships within the data. The network output layer comprised two nodes, corresponding to the classification categories: pure and adulterated honey, as illustrated in Fig. 3.

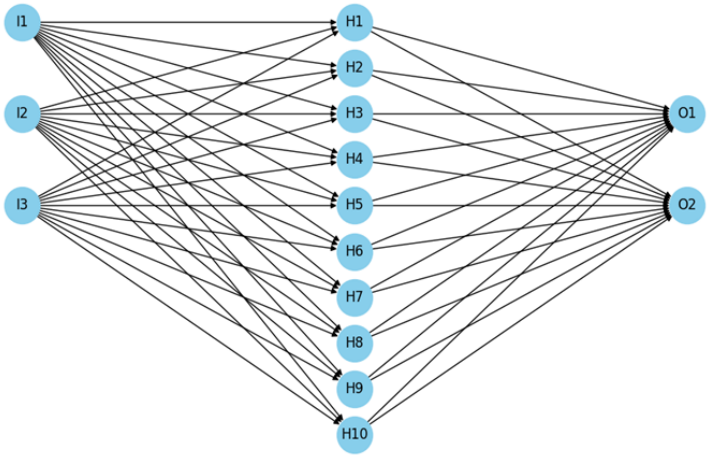

Fig. 3 *The ANN architecture*

The ANN was trained using a supervised learning approach with a labelled data set of pure and adulterated honey samples. Training utilized the back-propagation algorithm combined with gradient descent optimization to minimize classification errors. To ensure robustness and prevent over fitting, the data set was divided into training and validation subsets during the training process. After training, the ANN model was applied to classify unknown honey samples based on their spectral features. Model performance was evaluated using metrics such as accuracy, sensitivity, and specificity. This approach provides a rapid, non-destructive, and automated method for reliable honey authentication and adulteration detection.

4. Results and Discussion

4.1 Comparison of Absorbance and Transmittance Test Between Pure Honey and Diluted Honey

Fig. 4 illustrates the comparison of the absorbance signal response between pure honey and diluted honey across three measurement readings. Pure honey samples were loaded into a Quartz cuvette before being inserted into a spectroscopy meter for analysis. The results indicate a slightly higher absorbance signal response for pure honey compared to diluted honey. In the case of diluted honey, the absorption signal response shows a gradual decrease beginning at 350 nm wavelength and stabilizing at 560 nm wavelength. Conversely, pure honey samples exhibit a longer decay period starting at 410 nm wavelength and reaching stability at 560 nm wavelength, similar to diluted honey.

Both types of honey display a consistent signal pattern, with a slight undershoot response observed in the 950 nm to 980 nm wavelength range across all three measurement readings. This undershoot occurs between 930 nm and 980 nm wavelength for both pure honey and diluted honey, generating a comparable signal pattern. However, the absorbance signal for pure honey consistently registers a 0.14 higher signal response than diluted honey. Fig. 6 presents a comparative analysis of the absorbance signal responses between pure and diluted honey across three measurement trials. The samples of pure honey were loaded into quartz cuvettes and analysed using a UV-Vis spectrophotometer. The absorbance readings show that pure honey consistently exhibits a slightly higher signal response than diluted honey.

For diluted honey, the absorbance signal demonstrates a gradual decline beginning at approximately 350 nm and stabilizes near 560 nm. In contrast, pure honey shows a delayed decay in absorbance, initiating around 410 nm and also reaching a stable response at 560 nm, following a similar stabilization point to diluted honey. Both sample types exhibit consistent spectral patterns across all three measurements. Notably, a slight undershoot is observed in the 930–980 nm wavelength range for both pure and diluted honey. Despite the similarity in pattern, the absorbance signal of pure honey maintains an average response approximately 0.14 units higher than that of diluted honey throughout the spectral range.

J. of Electronic Voltage and Application Vol. 7 No. 1 (2026) p. 28-44

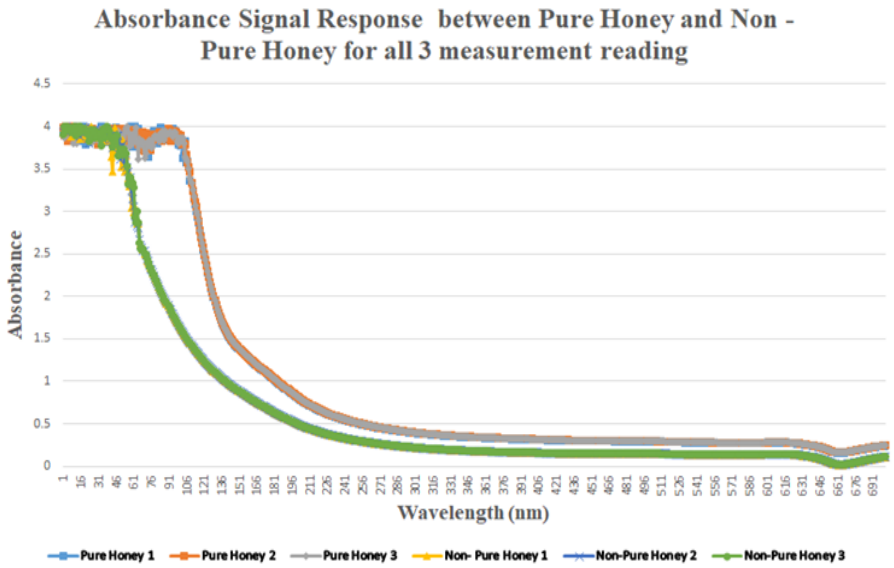

Fig. 4 *Absorbance signal response comparison between pure honey and diluted honey*

Fig. 5 shows the transmitted signal response between pure honey and diluted honey. In the case of diluted honey, the transmitted signal gradually increases from an initial level of 0 to 73.45 at a wavelength of 360 nm. Conversely, the pure honey sample exhibits a delayed increase, starting at 420 nm wavelength and reaching a transmitted level of 50.99 at 910 nm wavelength. The transmitted signal level is notably lower for pure honey compared to diluted honey, with a difference of 22.46.

The transmitted signal response for pure honey is consistently lower compared to diluted honey samples. Towards the end of the 1000 nm wavelength range, both pure honey and diluted honey show an over-damped curve, particularly evident from 920 nm onwards. However, the maximum peak level of the transmitted signal differs between the two types of honey. For non-pure honey, the maximum peak level reaches 99.51, whereas for pure honey, it peaks at 68.07. In summary, the transmitted signal response indicates that diluted honey exhibits higher levels compared to pure honey. Conversely, the absorbance response shows that pure honey has higher levels than diluted honey, resulting in an inverse relationship between the two types of honey in terms of these two signal parameters.

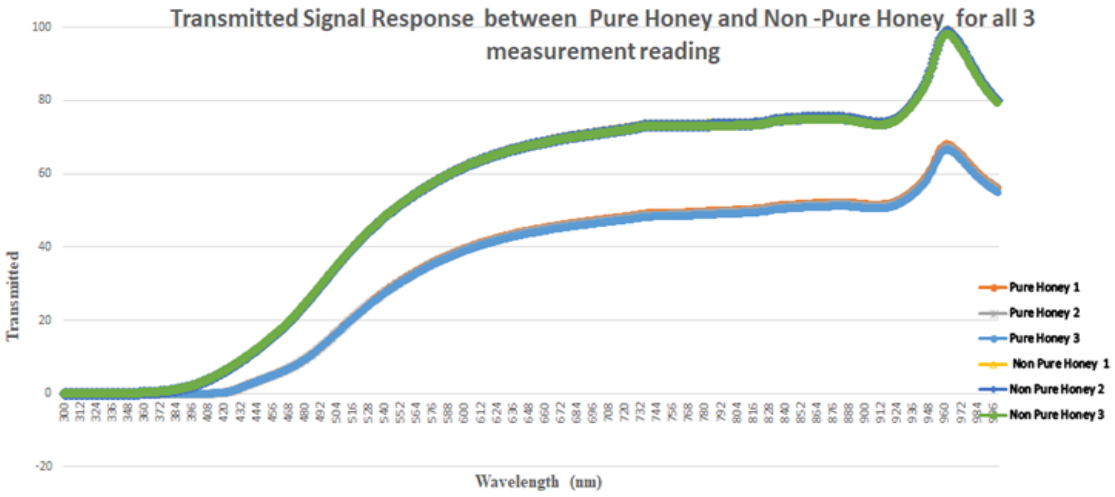

Fig. 5 *Transmitted signal response between pure honey and diluted honey*

4.2 Absorbance and Transmitted Signal For 8 Different Samples of Honey

Fig. 6 shows the absorption signal response for eight different honey samples. Each sample underwent individual testing, with honey placed in a cube-sized cuvette before insertion into the spectroscopy meter for measurement.

The displayed results indicate that pure honey exhibits a higher absorption rate, maintaining four levels of absorbance corresponding to different pure honey categories. The decrease in absorbance begins gradually, starting at 336 nm and continues until the wavelength was at 510 nm. A longer duration of honey maintaining a steady absorbance level signifies better quality, pure honey.

Among the samples, "Gold Ternak" shows an earlier decrease in absorbance compared to others, with a rapid transition at the steady state level of absorbance (A=4.0). "Black Seed Honey" follows, starting its decay at 331 nm wavelength and settling down at 870 nm before exhibiting a bumping signal at 970 nm wavelength. "Pure Gold K.L" decays proportionally to wavelength, saturating at certain points (e.g., 720 nm) before mirroring the bumping signal pattern at 970 nm wavelength. The "Pure Honey" and "Sik Honey" exhibit similar behaviour, settling at an absorbance level of 0, indicating reflection or transmission. "Kelulut_H" begins its decay at 306 nm wavelength, intersecting with "Pure Gold K.L" at 730 nm with an absorbance of 0.65. "Acacia Honey" maintains an absorbance rate of 4 until 473 nm wavelength before gradually decreasing, showing a bumping signal at 960 nm.

The "Tualang_H" represents the highest-quality pure honey, with its absorbance signal only starting to decay at 510 nm from the saturated 4 absorbance level. It exhibits sharp edges in the signal response, settling slowly at approximately 0 absorbance at 852 nm before a slight bump at 953 nm wavelength.

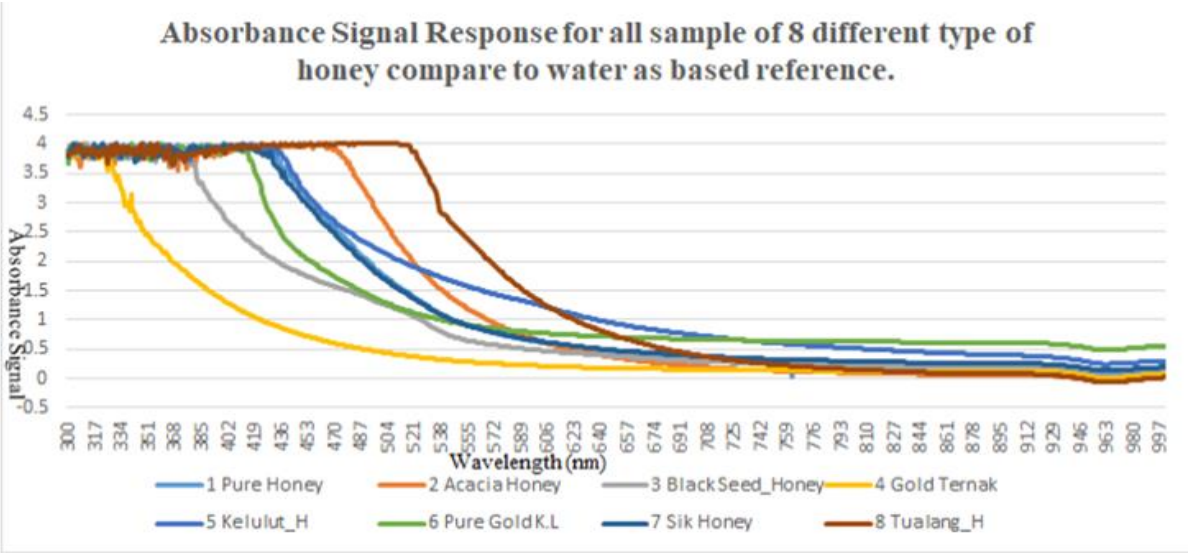

Fig. 6 *Absorbance signal response for 8 different samples of honey compared to water as a base reference*

Fig. 7 shows the transmitted signal response for eight different honey samples, measured by the spectroscopy meter. The results show that the transmitted signal for the purest honey takes longer to reach its peak compared to less pure or mixed honey samples, which serves as an initial screening test to distinguish between pure and adulterated honey. Among the eight samples of pure honey, "Pure Gold K.L Honey" exhibits a rapid increase in transmission starting at 340 nm wavelength, culminating in a peak transmitted signal level of 159.6 at 950 nm wavelength. Following this, "Black Seed Honey" shows a similar signal pattern, albeit slightly lower than "Pure Gold K.L Honey", with a peak transmitted signal level of 158.64 at 950 nm wavelength.

The "Pure Honey" starts to increase transmission at 415 nm wavelength after maintaining a 0 transmitted signal level, reaching a peak level of 92.44 at 961 nm wavelength. "Sik Honey" exhibits a comparable pattern but with a lower peak transmitted signal level of 87.32 at 962 nm wavelength. The transmitted signal for "Acacia Honey" increases significantly at 476 nm wavelength, peaking at 161.772 before decreasing to 132.35 at 961 nm wavelength. "Kelulut_Honey" and "Tualang_Honey" display intersecting signals, with "Kelulut_Honey" starting its increase at 436 nm wavelength and "Tualang_Honey" at 518 nm wavelength. "Kelulut_Honey" peaks at 71.85 at 962 nm wavelength, while "Tualang_Honey" peaks higher at 111.41 at 966 nm wavelength.

In summary, the transmitted signal responses indicate distinct patterns for each honey sample, with differences in peak levels and wavelengths of signal increase, providing insights into the purity and quality of the differences of honey samples.

J. of Electronic Voltage and Application Vol. 7 No. 1 (2026) p. 28-44

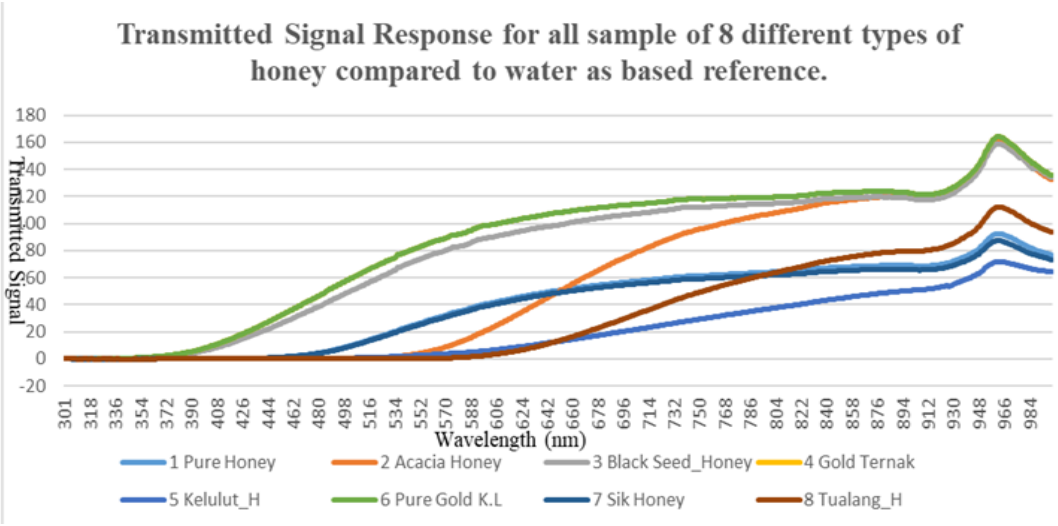

Fig. 7 *Transmitted signal response for 8 different sample of honey compare to water as based reference*

4.3 Sensitivity Test for Absorbance and Transmittance Wavelength

In theory, blue light typically corresponds to a shorter wavelength range spanning from 450 nm to 495 nm. The varying coloration of honey significantly influences the absorbance test, with factors such as floral origin or plant source, mineral content, phenolic compounds, storage conditions, and temperature which play crucial roles. The absorbance sensitivity within the wavelength range of 400 nm to 500 nm is directly related to honey compounds that absorb light, with blue-violet light absorption typically occurring around 480 nm, resulting in the distinctive orange-amber of honey. Higher absorbance intensities indicate darker sample colours, while lower intensities signify lighter shades. Among the honey samples analysed, the spectrum of "Tualang_Honey" demonstrates the highest intensity in this wavelength range, followed by "Acacia Honey," "Kelulut_Honey," "Pure Honey," "Sik Honey," "Pure Gold K.L Honey," "Black Seed Honey" and "Gold Ternak," as shown in Fig. 8. Increased absorbance levels generally indicate higher purity levels of honey. Additionally, for the green light of the laser, absorption occurs around 530 nm wavelength.

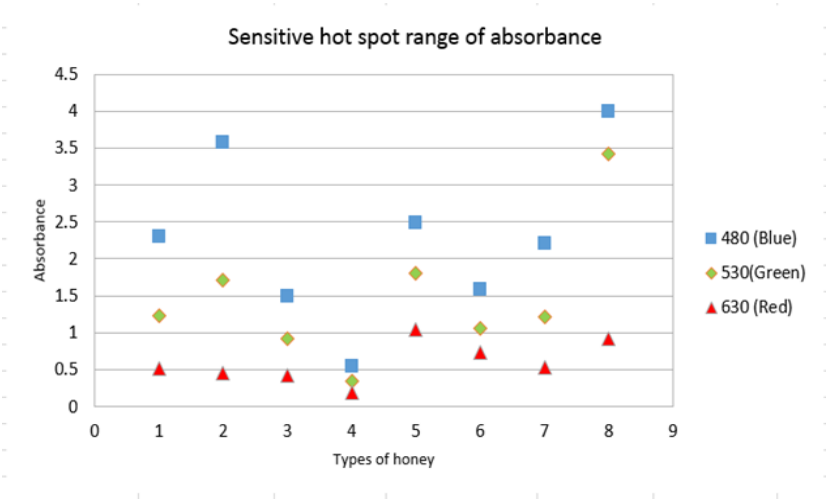

Fig. 8 *Sensitivity range of wavelength at 480 nm (blue), 530 nm (green) and 630nm (red) for absorbance test of 8 different samples of honey*

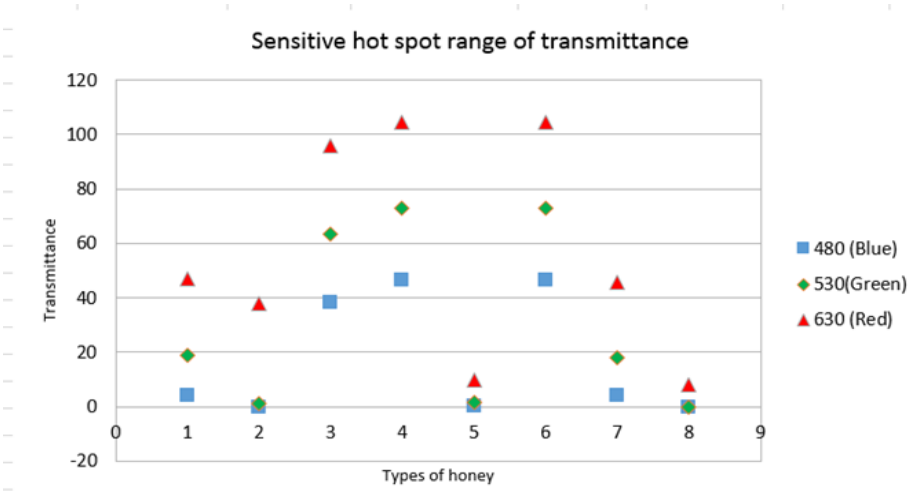

Fig. 9 *Sensitivity range of wavelength at 480 nm (blue), 530 nm (green) and 630nm (red) for transmittance test of 8 different samples of honey*

In terms of the transmitted test, the highly responsive areas for transmittance are identified at specific wavelengths: 480 nm for blue light, 530 nm for green light, and 630 nm for red laser light. Examining the graph presented in Fig. 9, the transmittance levels for "Pure Gold K.L Honey" and "Gold Ternak Honey" exhibit similarity, with a transmittance level of 46.56 observed at 480 nm wavelength (blue laser light), 72.97 at 530 nm wavelength (green laser light), and the highest level of signal response observed at 630 nm wavelength (red laser light) at 104.60. Hence, the transmitted signal response highlights three key wavelength points of sensitivity, necessitating a thorough investigation into the comparison between the optical design sensor and the measurement data from the MINT- SRC UTHM lab to ensure the comparability of results in identifying wavelength hotspots. The colours present in honey significantly impact the outcome of the measurement process.

It is worth noting that light interacts in three primary ways: absorption, reflection, and transmission. Typically, we observed transmitted light, and white light comprises a combination of seven distinct colours - violet, indigo, blue, green, yellow, orange, and red. As light waves traverse through a denser medium, their colour remains consistent while the speed decreases. The specific colour of light is determined by its wavelength, representing the distance between consecutive wave crests.

4.4 Absorbance and Transmitted Signal Response between Pure Tualang Honey (PTH) and Adulterated Tualang Honey (ATH)

This study investigates the optical characteristics of pure Tualang honey (PTH) and adulterated Tualang honey (ATH) using spectrophotometric methods, focusing on absorbance and transmission responses across the visible wavelength range of 400–500 nm. Fig. 10 shows that PTH consistently exhibits higher absorbance values than ATH across all wavelengths and measurement times. This indicates a greater presence of light-absorbing compounds in pure honey, such as flavonoids, phenolic acids, and other bioactive constituents. The absorbance curves for PTH are more pronounced and stable, suggesting a denser and chemically richer composition. In contrast, ATH shows lower absorbance, which may be attributed to dilution or the presence of non-natural additives that reduce the concentration of active compounds. Fig. 11 shows the result of the absorbance and transmitted signal responses, respectively, for both honey types over three measurement sessions.

J. of Electronic Voltage and Application Vol. 7 No. 1 (2026) p. 28-44

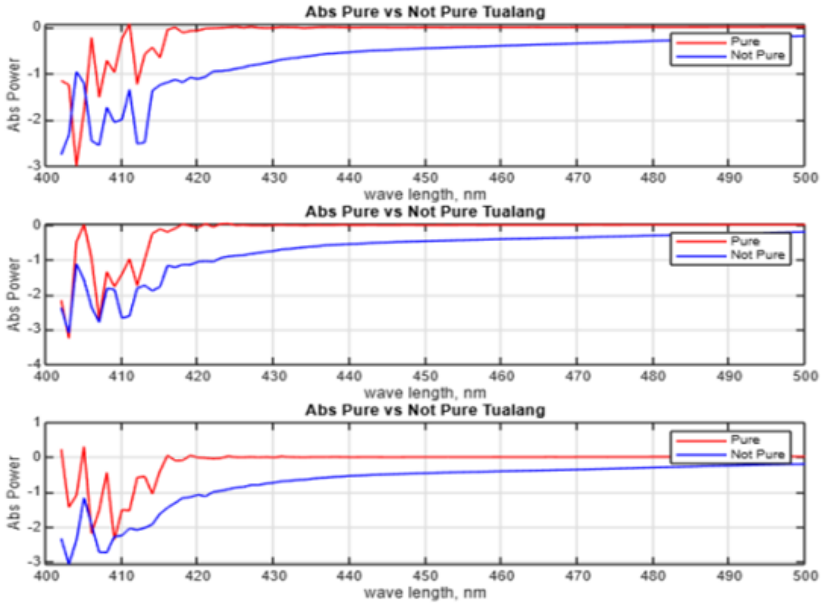

Fig. 10 *Absorbance signal response comparison between PTH and ATH for all 3 times of measurement reading*

Fig. 11 presents the transmission spectra, where ATH demonstrates higher transmitted signal intensity compared to PTH. This implies that ATH is more optically transparent, likely due to its lower concentration of suspended particles and solutes. The reduced transmission in PTH further supports its higher optical density and complex matrix, which scatters and absorbs more light.

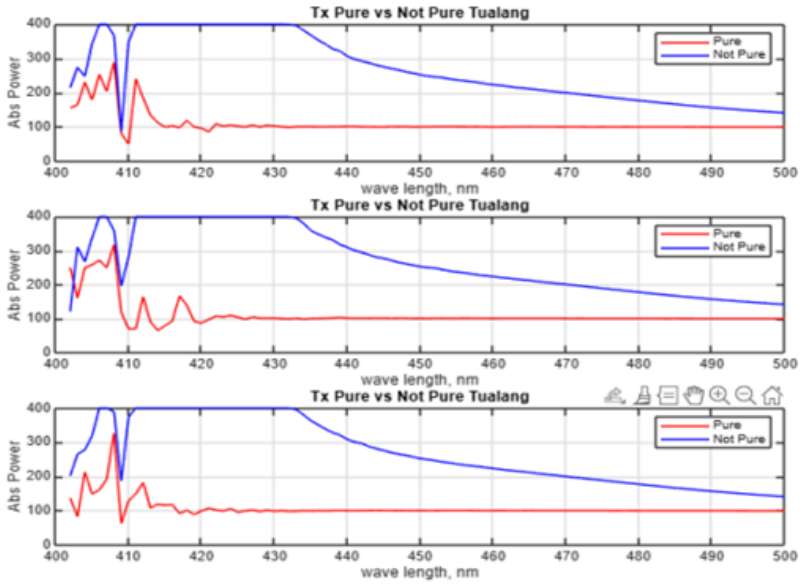

Fig. 11 *Transmitted signal response between PTH and ATH for all 3 times of measurement reading*

4.5 Application on Neural Networks on Simulation Analysis Result Using MATLAB

This experiment was further evaluated using neural networks through simulation analysis conducted in MATLAB. The simulation process involved modelling the data set into three subsets: training, validation, and test. As shown in Fig. 12, the training data set A consisted of 34 samples, while both the validation and test sets contained 7 samples each. The performance of the model was assessed using cross-entropy and error percentage metrics. The cross-entropy values recorded were 0.0874 for training, 0.1690 for validation, and 0.5058 for testing, indicating a progressive increase in loss from training to test, which may suggest over fitting. Similarly, the percentage of error increased from 0.0882 in training to 0.1429 in validation and 0.2857 in testing. These results highlight the model's reduced generalization capability on unseen data. Based on these metrics, confusion matrices were

plotted for each subset training, validation, and test—and subsequently combined into a single comprehensive plot, as illustrated in Fig. 6. This combined confusion matrix provides a visual summary of the model's classification performance across all data partitions.

Fig. 12 *Result using Neural Networks MATLAB data set A*

The training data set B consisted of 34 observations, the validation set included 7, and the test set comprised 8 observations. The model's performance was assessed using cross-entropy and error rate metrics. Remarkably, the cross-entropy values were extremely low — 4.2936e-07 for training, 7.8538e-07 for validation, and 9.7318e-07 for testing—indicating highly accurate predictions. Additionally, the error rate for all three subsets was 0, suggesting perfect classification during this simulation. Confusion matrices were generated for each subset to visualize classification accuracy. The training confusion matrix shows that Class A and Class B were correctly classified with high precision, while Class C had no recorded output, possibly due to data imbalance or absence in the training set. The validation and test confusion matrices were not fully populated, indicating either missing data or incomplete simulation output. To provide a comprehensive overview, all confusion matrices were combined into a single plot, as illustrated in Fig. 13, summarizing the model's classification performance across all data partitions.

Fig. 13 *Result using Neural Networks MATLAB data set B*

J. of Electronic Voltage and Application Vol. 7 No. 1 (2026) p. 28-44

Further analysis by training data set C consisted of 75 observations, the validation set included 17, and the test set comprised 10 observations. The model's performance was assessed using cross-entropy and error rate metrics. The cross-entropy values recorded were 0.0932 for training, 0.0942 for validation, and 0.0742 for testing, indicating consistent and relatively low loss across all subsets. The corresponding error rates were also low, suggesting good classification performance. All confusion matrices were combined into a single comprehensive visualization, as shown in Fig. 14 offering a complete overview of the model's classification performance across all data partitions.

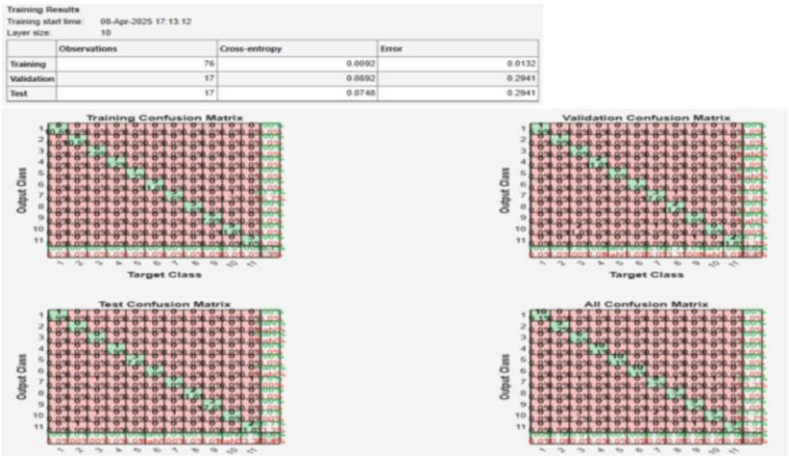

Fig. 14 *Result using Neural Networks MATLAB data set C*

Referring to Fig. 15, the data set labelled D was evaluated using a neural network model through simulation analysis in MATLAB. The data set was divided into three subsets: 76 samples for training, and 17 samples each for validation and testing. The model's performance was assessed using cross-entropy and error rate metrics. The cross-entropy values recorded were 0.0863 for training, 0.0894 for validation, and 0.0831 for testing, indicating consistent and low loss across all subsets. The percentage of error was 0.5000 for training and 0.6471 for both validation and test sets, suggesting a moderate level of misclassification.

Fig. 15 *Result using Neural Networks MATLAB data set D*

In Fig. 16, it can observe that the number of training is 34 and validation number is 8 and same as number of tests which is 8. Meanwhile for cross-entropy, the number of training is 3.0474e-07 and number of validations is 5.1815e-04. However, for the cross-entropy the number of tests is 6.6826e-05. For the percentage of error, we can see that the percentage of error is 0 for all the training, validation and test.

Fig. 16 *Result using Neural Networks MATLAB data set E*

Meanwhile, we will look on the neural networks data set F in Fig. 17, we can observe that the number of training is 34 and validation number is 8 and same as number of tests which is 8. Meanwhile for cross-entropy, the number of training is 1.8187e-07 and number of validations is 1.9505e-07. However, for the cross-entropy the number of tests is 1.9544e-07. For the percentage of error, we can see that the percentage of error is 0 for all the training, validation and test.

Fig. 17 *Result using Neural Networks MATLAB data set F*

In the final step of the analysis, neural network modelling was conducted using MATLAB to compare the classification performance between pure Tualang honey (PTH) and adulterated Tualang honey (ATH). The evaluation focused on key training metrics including performance, gradient, and validation checks. Initially, the performance value was 0.596, which progressively decreased to a stop value of 0.0502, with a target value of 0, indicating successful error minimization during training. The gradient value started at 0.72 and reduced to 0.033, approaching the target threshold of 1e-06, suggesting stable convergence of the model parameters. For the validation check, the process began at 0, and reached a stop value of 6, which matched the target value, indicating that the model stopped training after six consecutive validation failures, a common early stopping criterion to prevent over fitting. From this network training analysis, several diagnostic plots were generated, including the performance plot, gradient plot, and validation check plot, which collectively illustrate the learning dynamics of the model. Additionally, the confusion matrix was plotted to evaluate classification accuracy across different classes. To further compare the performance between PTH and ATH, the best validation performance graph was plotted as shown in Fig. 18, while the error histogram with 20 bins was illustrated in Fig. 19, providing a detailed view of prediction errors and their distribution across the data set.

J. of Electronic Voltage and Application Vol. 7 No. 1 (2026) p. 28-44

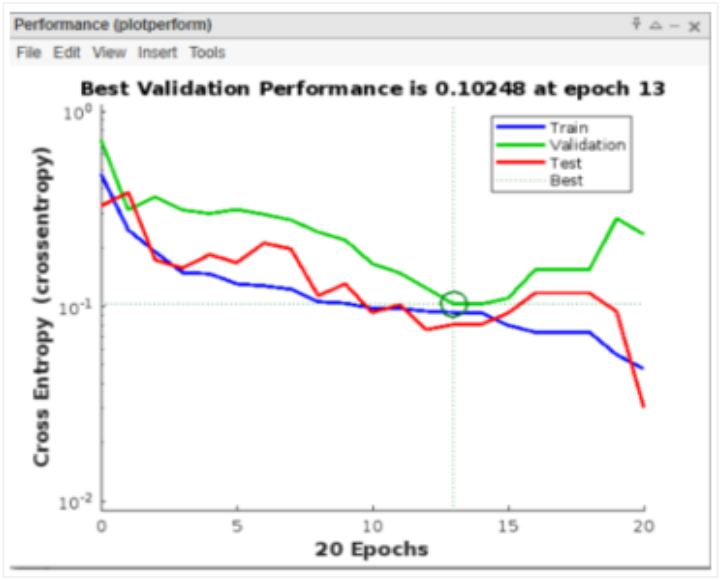

Fig. 18 *Graph of best validation performance to compare between PTH and ATH*

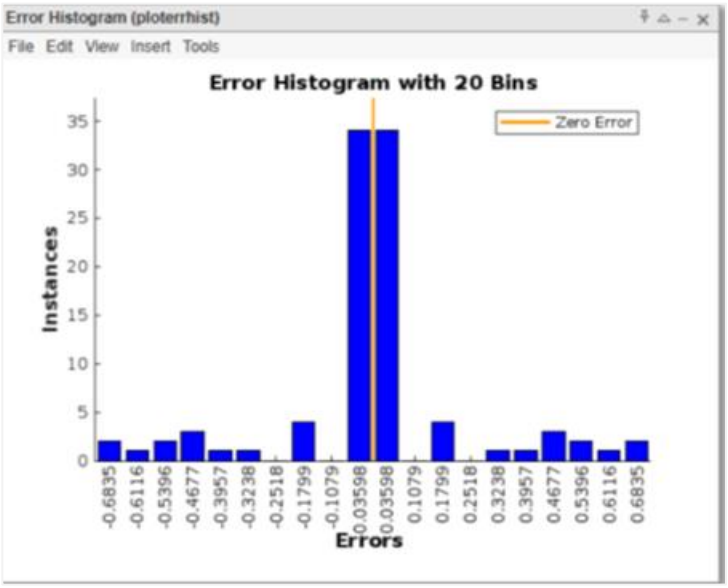

Fig. 19 *Graph of error histogram with 20 bins to compare between PTH and ATH*

The confusion matrix presented provides a summary of the classification performance of the neural network model in distinguishing between pure Tualang honey (PTH) and adulterated Tualang honey (ATH). The matrix shows that the model correctly classified 85.4% of the samples, while 14.6% were misclassified. This indicates a high level of accuracy in the model's predictions, with the majority of output classes aligning with their respective target classes. The remaining 14.6% represents instances where the model failed to match the predicted class with the actual class, which may be attributed to overlapping features or noise in the dataset. Overall, the confusion matrix confirms that the neural network demonstrates strong classification capability in differentiating between PTH and ATH.

5. Conclusion

This study explored the issue of honey adulteration and reviewed various detection techniques, with a specific focus on optical methods. Using a UV-Vis spectrometer, clear distinctions were observed between pure and ATH samples based on their absorbance and transmittance characteristics. The results indicated that darker honey exhibited higher absorbance at 480 nm, while lighter honey responded more rapidly in transmittance measurements, particularly at 630 nm. These findings demonstrate the potential of UV-Vis spectroscopy as a

simple, rapid, and cost-effective method for assessing honey purity [20]. The insights gained from this work contribute to ongoing efforts in developing accessible tools for honey authentication and offer a foundation for future research in optical sensing techniques for food quality assessment.

Besides, this study successfully demonstrated the application of spectrophotometric and neural network-based analysis to differentiate between pure Tualang honey (PTH) and ATH. Spectrophotometric results showed consistent differences in absorbance and transmission characteristics, with PTH exhibiting higher absorbance and lower transmission across the 400–500 nm wavelength range, indicating a denser and more complex composition. Further evaluation using neural network simulations in MATLAB provided strong classification performance. Across multiple datasets, the models achieved low cross-entropy values and minimal error rates, with some configurations reaching 0% classification error. Confusion matrices confirmed high accuracy, with the best model achieving 85.4% correct classification. Additional performance metrics, including gradient descent behaviour, validation checks, and error histograms, supported the model's robustness and convergence. Overall, the integration of optical analysis and neural network modelling proved to be an effective, non-destructive approach for honey authentication. These findings contribute to the development of reliable quality control methods in the food industry, particularly for detecting honey adulteration.

Acknowledgement

This research is supported by Universiti Tun Hussein Onn Malaysia under the REGG grant number Q040.

Conflict of Interest

Authors declare that there is no conflict of interests regarding the publication of the paper.

Author Contribution

The authors are responsible for the study conception, research design, data collection, data analysis, result interpretation and manuscript drafting.

References

[1] Molan, Peter C. "The antibacterial activity of honey: 1. The nature of the antibacterial activity." *Bee world 73.1* (1992): 5-28.

[2] Cooper, Rose A., Peter Charles Molan, and K. G. Harding. "Antibacterial activity of honey against strains of Staphylococcus aureus from infected wounds." *Journal of the royal society of medicine 92.6* (1999): 283-285.

[3] Blasa, Manuela, et al. "Honey flavonoids as protection agents against oxidative damage to human red blood cells." *Food chemistry 104.4* (2007): 1635-1640.

[4] Yusoff, K. M., Hamid, J. and Manap, M. N. A. (2006). The presence of synthetic and adulterated honeys in Malaysia. Abstracts of the 1st International Conference on the Medicinal Uses of Honey (from Hive to Therapy). August 26–28, 2006. Kelantan, Malaysia: *Malaysian Journal of Medical Sciences, 123.*

[5] Bertelli, Davide, et al. "Detection of honey adulteration by sugar syrups using one-dimensional and two-dimensional high-resolution nuclear magnetic resonance." *Journal of agricultural and food chemistry 58.15* (2010): 8495-8501.

[6] Zhu, Xiangrong, et al. "Detection of adulterants such as sweeteners materials in honey using near-infrared spectroscopy and chemometrics." *Journal of Food Engineering 101.1* (2010): 92-97.

[7] Zakaria, Ammar, et al. "A biomimetic sensor for the classification of honeys of different floral origin and the detection of adulteration." *Sensors 11.8* (2011): 7799-7822.

[8] Tosun, Murat. "Detection of adulteration in honey samples added various sugar syrups with 13C/12C isotope ratio analysis method." *Food chemistry 138.2-3* (2013): 1629-1632.

[9] Wang, Shaoqing, et al. "Detection of honey adulteration with starch syrup by high performance liquid chromatography." *Food chemistry 172* (2015): 669-674.

[10] Subari, Norazian, et al. "A hybrid sensing approach for pure and adulterated honey classification." Sensors 12.10 (2012): 14022-14040.

[11] M.B. Jaafar, M. B. Othman, M. Yaacob, B.A. Talip, M.A. Ilyas, N.H Ngajikin, N.A. M. Fauzi, "A Review on Honey Adulteration and The Available Detection Approaches", *International Journal of Integrated Engineering* Vol 12 No. 2 (2020) 125-131.

[12] Hida, N., Abdullah, M., & Yasin, M. (2015). Fiber Optics Displacement Sensor for Honey Purity Detection Using Glucose Adulteration. *Journal Teknologi*,74(8). https://doi.org/10.11113/jt. v74.4711.

[13] Rajalakshmi, G., et al. "Identification of moisture, glucose, sucrose, fructose region in honey sample using NIR spectroscopy." 2017 Third International Conference on Sensing, Signal Processing and Security (ICSSS). IEEE, 2017.

[14] Lekova, Svetla, and Diana Tsankova. "Determination of botanical origin of honey by mid infrared spectroscopy (mid-FTIR), colorimetry and chemometric analysis." *Journal of Chemical Technology and Metallurgy 52.1* (2017): 52-57.

[15] Sivakesava, S., and J. Irudayaraj. "Prediction of inverted cane sugar adulteration of honey by Fourier transform infrared spectroscopy." *Journal of food science 66.7* (2001): 972-978.

[16] Kumaravelu, C., and A. Gopal. "A review on the applications of Near-Infrared spectrometer and Chemometrics for the agro-food processing industries." 2015 *IEEE Technological Innovation in ICT for Agriculture and Rural Development (TIAR)* (2015): 8-12.

[17] Perrotti, Angelina G., et al. "Efficacy of sonication-assisted sieving on Quaternary pollen samples." *Palynology 42.4* (2018): 466-474.

[18] Gallina, Albino, Nicoletta Stocco, and Franco Mutinelli. "Karl Fischer Titration to determine moisture in honey: A new simplified approach." *Food Control 21.6* (2010): 942-944.

[19] Isengard, Heinz-Dieter, et al. "Alternatives to official analytical methods used for the water determination in honey." *Food Control 12.7* (2001): 459-466.

[20] I. Karabagias, C. Kontakos, and A. Drouzas, "Characterization and classification of honeys by UV spectroscopy and multivariate analysis," *J. Food Sci. Technol.*, vol. 55, no. 12, pp. 4861–4870, 2018.